Analysis of Truncated Periodic Array Using Two-Stage Wavelet-Packet Transformations for Impedance Matrix Compression

Yair Shifman, *Student Member, IEEE*, Zachi Baharav, and Yehuda Leviatan, *Fellow, IEEE*

***Abstract*— A novel method of moments procedure is applied to the problem of scattering by metallic truncated periodic arrays. In such problems, the induced current shows localized behavior within the unit cell and at the same time exhibits cell-to-cell periodicity. In order to select a set of expansion functions that may account for such behavior, a two-stage basis transformation, of which the first stage is an ordinary wavelet transformation performed independently on each unit-cell, has been applied to a pulse basis. The resultant basis functions at the first stage are regrouped and retransformed to reveal the periodicity of their coefficients. Expansion functions are then iteratively selected from this newly constructed basis to form a compressed impedance matrix. The compression ratios obtained in this manner are higher than the compression ratio achieved using a basis constructed via an ordinary single-stage wavelet transformation, where compression is the ratio between the number of nonzero elements in the matrix used to solve the problem and the number of elements in the original matrix. An even higher compression is attained by considering, in addition, functions that reveal array-end related features and iteratively selecting the expansion from an overcomplete dictionary.**

***Index Terms*— Electromagnetic scattering by periodic structures, method of moments, wavelet transforms.**

I. Introduction

AMONG the various categories of scattering problems the case of scattering by a truncated periodic array is of special challenge to be efficiently solved. Such arrays are widely used in both microwave and optical systems owing to their frequency selective properties. Their various applications range from microwave filters to optical focusing devices and reflectors. In a strictly periodic case it is possible to define a unit cell, which once analyzed reveals the entire information about the scattered fields. Unfortunately, in a real case, edge-effects break down the pure periodicity.

Various authors [1]–[3] have proposed methods for solving these scattering problems, which involve some kind of approximation or modification of the Floquet modes in order to compensate for the truncation of the infinite array. The method proposed in this paper is motivated by the fact that in such problems the induced surface current might exhibit complicated localized behavior within the unit-cell while keeping a certain degree of cell-to-cell periodicity. We therefore construct a new set of expansion functions for the scattering equation via a two-stage transformation. Of these two stages, the first one is carried out at the unit-cell level and focuses on the localized features of the current. We have chosen to apply the wavelet transformation at this stage, owing to its multiresolution property that enables efficient expansion of the solution of scattering problems [4]. The transformation is applied to each cell as if it were isolated from the others, therefore excludes wavelet functions that span over more than one cell. The second stage is performed at the array-level and binds together identical basis functions from different cells, thereby taking into account the inherent periodicity of the array. Assuming that the cells are similar (let alone identical), we expect the same basis functions to be the dominant one in each and every cell. Hence, the second stage of transformation is expected to result in a new basis comprising composite functions which are much more suitable for effectively expanding the current.

Once this new basis has been constructed, we can apply the impedance matrix compression (IMC) and more particularly the iterative IMC methods presented in [5]–[8]. These methods solve a reduced (compressed) version of the matrix form of the corresponding electromagnetic field integral equation. The reduced form is obtained via an iterative process that extracts a set comprising a small number of basis elements for expanding the solution at a given accuracy. We further note that the cell-to-cell variation of the coefficients of identical basis functions belonging to different cells is expected to be mainly characterized by phase-alternation. Therefore, it is very likely that a Fourier-like basis would be quite adequate for the second transformation stage. We have chosen to use the windowed-Fourier-transform wavelet-packet (WF) basis ([7], [9]). The elements of the WF basis may be well associated with a different equally-spaced nonoverlapping spatial frequency bands corresponding to the number of zero crossings they make, thus spanning the discrete spatial-frequency domain in a similar way to the discrete windowed (noncyclic) Fourier transform basis. Moreover, this basis has a simple transformation algorithm similar to the one used for wavelet transformation. We further note that edge-effects, due to the fact that the array is finite, call for more localized basis functions. Hence, both a WF and a wavelet transformation are applied independently at this second stage to form an overcom-

Manuscript received December 29, 1997; revised July 15, 1998. This work was supported in part by the Fund for Promotion of Research at the Technion.

The authors are with the Department of Electrical Engineering, Technion—Israel Institute of Technology, Haifa 32000, Israel (e-mail: leviatan@ee.technion.ac.il).

Publisher Item Identifier S 0018-926X(99)04768-7.

plete dictionary of expansion functions [10]. Performing the iterative matrix compression by selecting expansion functions from this dictionary improves the matrix compression.

The mathematical formulation of the problem and the newly proposed two-stage transformation are presented in the next section, followed by a thorough description of the iterative IMC method in Section III. The new approach has been successfully applied to the problem of two-dimensional (2-D) TM scattering by a finite periodic array of conducting strips, of which results are given in Section IV. The advantages of using the overcomplete set of wavelet-packet expansion functions are presented as well. Summary and conclusions are given in Section V.

II. Formulation

The general problem under consideration is that of evaluating the current density J_z on a truncated periodic array consisting of K perfectly conducting 2-D cylindrical scatterers excited by a time-harmonic TM_z wave. We first consider the following E-Field integral equation formulation [11]:

$$\frac{\omega\mu_0}{4}\int_C J_z(c')H_0^{(2)}(k_0|c-c'|)\,dc' = E_z^{\text{inc}}(c), \quad c\in C \tag{1}$$

where C is the contour of the K scatterers, ω is the frequency, k_0 is the wavenumber, and μ_0 is the permeability of vacuum. Equation (1) is then reduced to matrix form by expanding the current in terms of N pulse expansion functions and using $M(M\geq N)$ pulse testing functions. The result is

$$[Z]\vec{I} = \vec{V} \tag{2}$$

where $[Z]_{M\times N}$ is the MoM impedance matrix, $\vec{I}$ is the yet-to-be-determined current vector, and $\vec{V}$ is the excitation vector. Due to the use of pulse expansion and testing functions, the matrix $[Z]$ in (2) is inherently dense. With a view toward obtaining a reduced-rank (compressed) representation of (2), we seek a new basis $\{\mathcal{J}_i\}_{i=1}^N$, out of which a small number of selected functions would span the unknown induced current to a good accuracy. In this new basis, (2) takes the form

$$[\hat{Z}]\vec{\mathcal{I}} = \vec{V}. \tag{3}$$

Each column of $[\hat{Z}]$ describes the field across the array due to a different expansion function, and $\vec{\mathcal{I}}_{N\times 1}$ denotes the new vector of coefficients. The current density J_z is given in terms of the new basis functions as

$$J_z = \sum_{i=1}^{N}\mathcal{I}_i\mathcal{J}_i. \tag{4}$$

As candidates for new basis functions, we consider the use of multiresolution wavelet and wavelet-packet bases ([4], [10]). Yet, for a problem involving a finite array of scatterers these bases might not be good enough for our purposes, since an expansion of the induced current on the perimeter of each and every array element may require a large number of such functions. Therefore, we resort to our understanding of the characteristics of the induced current which stem from the periodicity of the scatterer. First, we expect to find the same dominant expansion functions on each of the various strips. Second, we expect the coefficients of respective expansion functions, each belonging to a different strip, to be characterized by a certain periodicity. Based on this observation, we suggest a new transformation technique that avails the periodic properties of the problem.

The basis construction proceeds as follows. First, we transform the $P=\frac{N}{K}$ pulse expansion functions within each unit-cell to P wavelet functions. This transform is effected, when using Haar wavelets, by terminating the transformation of the entire N pulse-function set at the $\log_2(P)$ level of the filter-tree. Hence, at the end of the first transformation stage the current in each cell is expanded by a similar set of wavelet expansion functions. We denote the set of wavelet functions associated with the kth unit-cell by $\{W_{p,k}^{\text{I,WL}}\}_{p=1}^P$, where the double superscript I, WL designates that these functions are associated with the first transformation stage and that the transformation is a wavelet one. Next, we group the wavelet functions from the various K unit-cells in P subsets, each comprising K similar wavelet functions, defined as

$$W_p^{\text{I}} = \{W_{p,k}^{\text{I,WL}}\}_{k=1}^K, \qquad p=1,\cdots,P \tag{5}$$

and in turn apply a WF transformation to the coefficients of each of these subsets. This second stage of ransformation is a procedure somewhat similar to extracting an array factor, and it yields, respectively, P subsets, each comprising K new basis functions which are linear combinations of similar wavelet functions belonging to different unit-cell. We denote these new basis functions by

$$W_p^{\text{II,WF}} = \{W_{p,k}^{\text{II,WF}}\}_{k=1}^K, \qquad p=1,\cdots,P \tag{6}$$

where the double superscript II, WF designates that these functions are associated with the second transformation stage and that the transformation is a windowed-Fourier-transform wavelet-packet one. Finally, these new basis functions are reordered using a single index for use in (4). That is

$$\mathcal{J}_i = W_{p,k}^{\text{II,WF}},$$
$$i = k+(p-1)\times K, \qquad k=1,\cdots,K,\ p=1,\cdots,P. \tag{7}$$

The idea is schematically illustrated in Fig. 1, where the same wavelet function participates in the expansion of the current on each one of the four scatterers. Since only the sign of the coefficients of these identical wavelet functions alternates, it is possible to describe this localized behavior of the current using merely one composite function instead of four: the fundamental wavelet function modulated by a periodic function accounting for the sign alternation. Hence, we can expect that a basis constructed in this manner will offer a considerably more concise expansion of the induced current.

It is possible to choose yet a more adequate basis for the problem by selecting it from an overcomplete dictionary [12]. An overcomplete dictionary $\mathcal{D}$ is defined as a family $\mathcal{D}=\{\mathcal{J}_\gamma\}_{\gamma\in\Gamma}$ of expansion functions of unit norm, where Γ is the set of indexes that uniquely define the dictionary elements. $\mathcal{D}$ contains at least one basis for the space spanned by the N pulse expansion functions. Again, for simplicity, we assume that the wavelet transformation is adequate enough

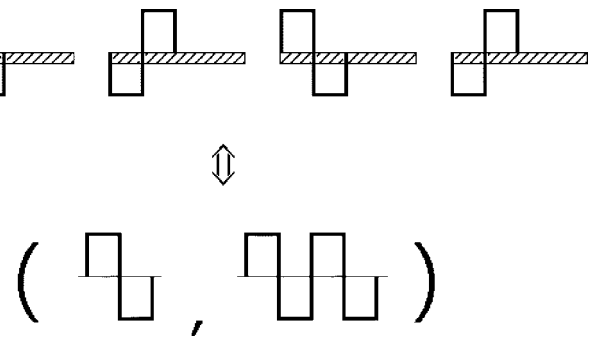

Fig. 1. The two-stage transformation. Four wavelet functions, each of which is used for expanding the current on a different strip, can be represented by a single composite function. This composite function is defined by the original wavelet function and the periodic function which describes the modulation of the wavelet function from one strip to the other.

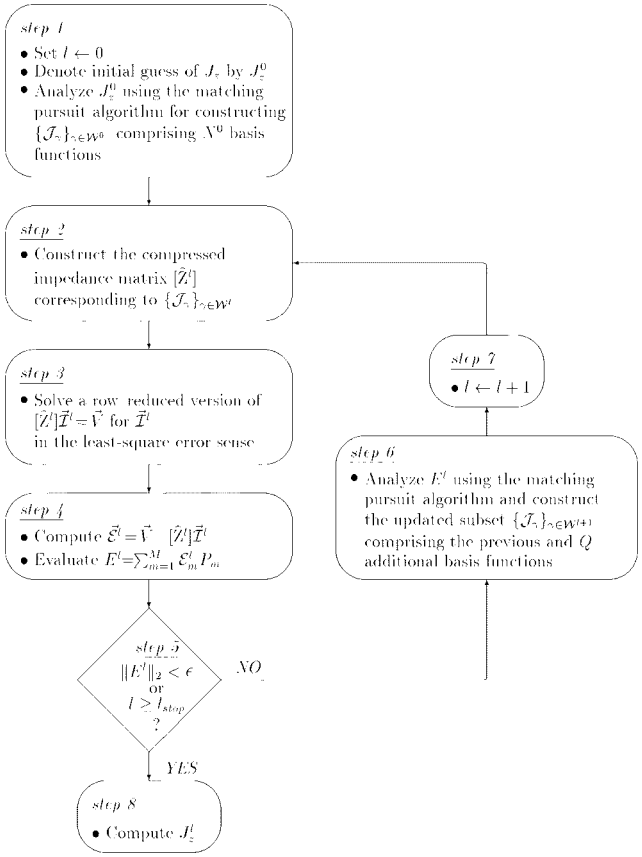

Fig. 2. Iterative algorithm for selection of expansion functions from an overcomplete dictionary.

for efficiently spanning the induced current on each array element. If the latter assumption does not hold, it is possible to start with an overcomplete dictionary as early as at the first transformation stage, at the expense of increased complexity. Regarding the second transformation stage, it is easy to realize that the WF transformation would not be the best choice. Specifically, periodicity no longer exists at the vicinity of the edges of a finite array of several wavelengths long. Therefore, WF functions fail to efficiently span the induced current there, hence a more localized basis is sought. We conclude by stating that selecting expansion functions from an overcomplete dictionary consisting of both WF and wavelet bases would yield a highly compressed matrix. Introducing the notation $W_p^{\mathrm{II,WL}}$ for the functions obtained when the transformation in the second stage is a wavelet one, the overcomplete dictionary, $\mathcal{D}$, for this case is defined as

$$\mathcal{D} = \{W_p^{\mathrm{II,WL}}\}_{p=1}^{P} \cup \{W_p^{\mathrm{II,WF}}\}_{p=1}^{P}. \tag{8}$$

III. The Iterative IMC Method

With a view toward reducing the number of basis functions needed while keeping the desired level of accuracy, an alternative solution technique for (3) has been proposed in [5], where a reduced (compressed) version of the linear equation is constructed and solved. For the construction of this compressed equation merely the dominant expansion functions of the solution are taken into consideration. Obviously these dominant functions are not known *a priori*. However, they can be obtained to a certain degree of success via an analysis of an initial guess for the solution such as the physical optics approximation. The analysis is performed either via the wavelet transformation as done in [5], or any other basis transformation. Adaptive analysis methods, such as best-basis analysis [6] can be incorporated for enhanced compression. Clearly, the analysis of an initial guess for the solution results in merely a crude approximation for the expansion subset of the exact solution. To improve the selection of a subset of dominant expansion functions, an iterative matrix construction process has been suggested in [8].

The complete iterative selection algorithm is shown in Fig. 2. Assuming N^l expansion functions have been chosen so far, we construct and solve in iteration l the reduced version of (3)

$$[\hat{Z}^l]\vec{\mathcal{I}}^l = \vec{V} \tag{9}$$

for $\vec{\mathcal{I}}^l$ in the least square error sense. The columns of $[\hat{Z}^l]$ describe the field across the array due to the N_l expansion functions, where the corresponding vector of coefficients is denoted by $\vec{\mathcal{I}}^l_{N^l \times 1}$. The indexes of the N^l independent elements of $\mathcal{D}$ that are used to construct $[\hat{Z}^l]$ are registered in a working subset $\mathcal{W}^l \subset \Gamma$. The compressed matrix equation (9) can be solved directly, but to further reduce the computational cost it can be solved by an iterative solver using $\vec{\mathcal{I}}^{l-1}$ as the initial guess for $\vec{\mathcal{I}}^l$. The vector of error coefficients is given by

$$\vec{\mathcal{E}}^l = \vec{V} - [\hat{Z}^l]\vec{\mathcal{I}}^l \tag{10}$$

and the boundary condition error can be readily evaluated as

$$E^l = \sum_{m=1}^{M} \mathcal{E}_m^l P_m \tag{11}$$

where $\{\mathcal{E}_m^l\}_{m=1}^{M}$ are the elements of $\vec{\mathcal{E}}^l$, and P_m denotes the mth function in the original pulse basis used for testing. An analysis of E^l is then used for adding new expansion functions for the construction of $[\hat{Z}^l]$ in the following iteration. This analysis is performed via projecting the error onto the residual elements (elements yet neither selected nor rejected) of the dictionary. Then, Q dominant elements are selected while

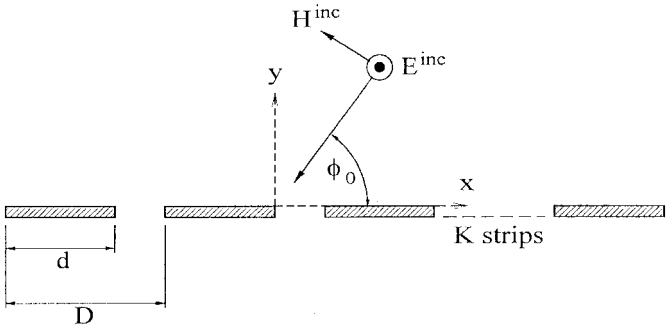

Fig. 3. Scattering problem of an array of conducting strips excited by an obliquely incident TM_z plane wave. Each strip is infinite in the z direction, while its thickness in the y direction is negligible.

rejecting those which are linearly dependent on the previously selected ones. At the end of each iteration, the current density J_z^l can be expressed according to

$$J_z^l = \sum_{\gamma \in \mathcal{W}^l} \mathcal{I}_\gamma^l \mathcal{J}_\gamma. \tag{12}$$

The iterative procedure terminates if either $\|E^l\|_2$ is smaller than a predefined value ϵ, or the iteration count has exceeded a predefined number $l_{\text{stop}} \leq N$. Note that instead of solving the original large matrix, we solve successively a series of compressed matrix-equations with a view toward attaining suitable accuracy more efficiently. It is possible to further lessen the computational complexity by reducing the number of rows of $[\hat{Z}^l]$ and $\vec{V}$ thus solving a row-reduced version of (9), keeping in mind, though, that to ensure stability, a certain ratio between the number of rows and columns is always maintained. In the first few iterations, the number of testing functions can be reduced even below the limit set by the sampling theorem for obtaining an accurate final solution since merely low-spatial-frequency functions are expected to be dominant. In the later iterations, sampling requirements should be fulfilled, and usually twice as many testing functions are used to ensure numerical stability. The implementation of an iterative selection of expansion functions from an overcomplete dictionary requires monitoring the linear independence of the selected functions as well as overcoming the difficulties introduced by their nonorthogonality. For this purpose, a version of the matching pursuit algorithm [12] has been adapted.

IV. Numerical Results

The example under consideration is the problem of scattering by an array of perfectly conducting 2-D strips, as shown in Fig. 3. There are $K = 16$ strips of $d = 2\lambda$ width. The spacing between the strips is $\lambda(D = 3\lambda)$, and an incident angle $\Phi_0 = 60°$ has been chosen. Thus a phase advancement of π radians from cell to cell is effected as $k_0 D \cos\Phi_0 = \frac{2\pi}{\lambda} \times 3\lambda \times \cos(60°) = 3\pi$. The discretization to pulses is done using 8 pulses per wavelength, or 16 pulses per strip, which amounts to a total of $N = 256$ pulses. To ensure numerical stability, twice as many testing points are used. Hence the dimension of the noncompressed impedance matrix is 512 × 256. We select $Q = 4$ additional expansion functions at each iteration. The amplitude and phase of the induced current for this problem are shown in Fig. 4. Note the rather complex behavior of the current on each strip and the periodicity that breaks down at the vicinity of the array edges. To demonstrate the advantage of the proposed method,

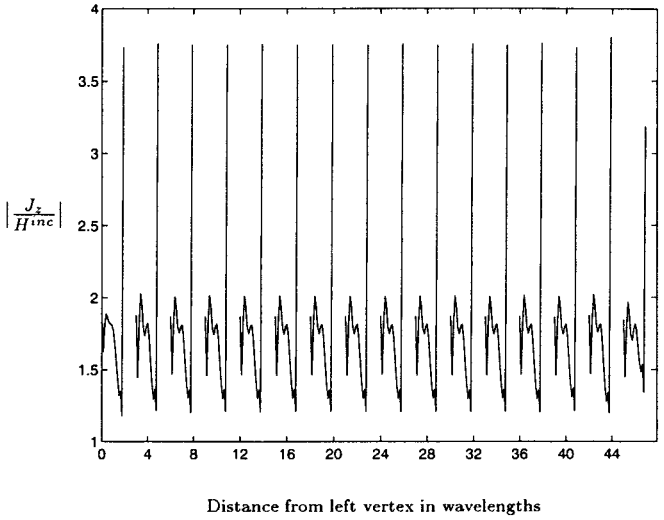

(a)

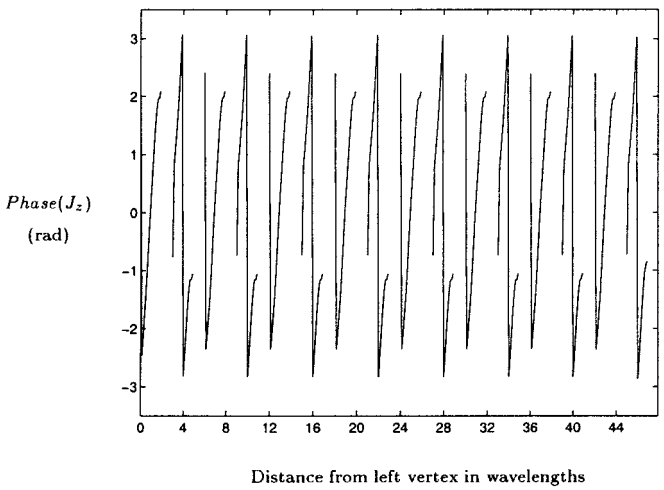

(b)

Fig. 4. Induced current density on the conducting strip, for the scattering problem illustrated in Fig. 3 obtained with 256 basis functions. (a) Magnitude. (b) Phase.

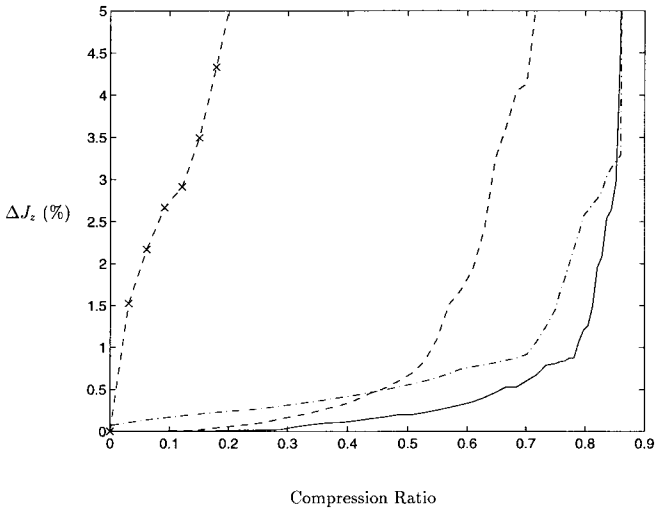

Fig. 5. Error in induced current density versus compression ratio, for the scattering problem illustrated in Fig. 3. Iterative selections were made from three different 2-D dictionaries, constructed via Haar wavelet transformation (first stage) and: Haar wavelet transformation (- - -), Haar WF (- · -), both transformations (-). A 512 × 256 reference impedance matrix is assumed. For comparison, the left-most graph (- × -) is the compression achieved by iterative selection from an ordinary Haar wavelet basis.

three expansion sets have been constructed in the following manner. The first transformation stage, for all three sets, was a Haar wavelet transformation up to level $\log_2(\frac{256}{16}) = 4$ of the wavelet filter-tree. We then construct two expansion sets by separately applying a second Haar wavelet and Haar WF transformations. The third set is an overcomplete dictionary comprising both of the above two individual sets. Denoting the number of rows in the row-reduced version of $[\hat{Z}^l]$ and $\vec{V}$ by M^l, the impedance matrix compression level attained is measured by the compression ratio evaluated as

$$\text{Compression Ratio} = 1 - \frac{M^l N^l}{MN}. \tag{13}$$

Fig. 5 shows the two-norm error in the induced current as a function of the compression ratio, computed according to

$$\Delta J_z(\%) = 100 \times \frac{\left\| J_z - J_z^{\text{REF}} \right\|_2}{\left\| J_z^{\text{REF}} \right\|_2} \tag{14}$$

where J_z^{REF} is a reference current obtained by solving (2) with the full 512 × 256 matrix. The three graphs on the right correspond to iterative selection of expansion functions from the three expansion sets defined above. For comparison, the left-most graph displays the compression ratio obtained by iterative selection from ordinary single-stage Haar wavelet transformation expansion functions. It is evident that the selection from the overcomplete dictionary yields the highest compression ratio, owing to its ability to span both periodic and localized features of the current.

More insight into the selection from the overcomplete dictionary discussed above can be gained by examining Fig. 6(a) and (b). Each one of these figures refers to a different basis: Fig. 6(a) is related to the basis constructed via applying the Haar wavelet transformation at both stages, while Fig. 6(b) is related to the basis constructed via first applying the

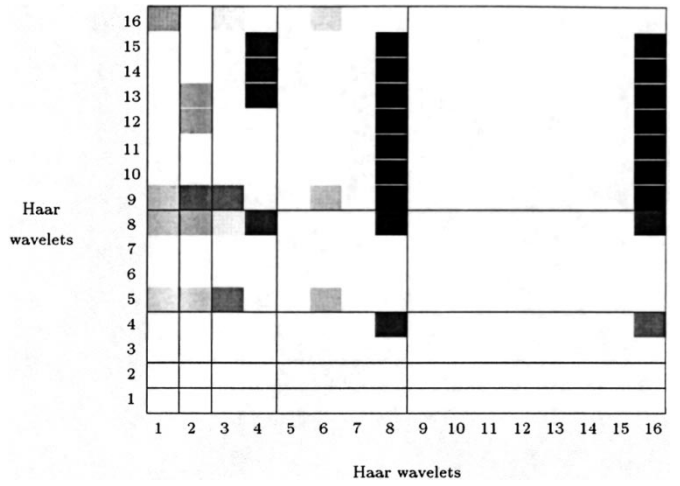

(a)

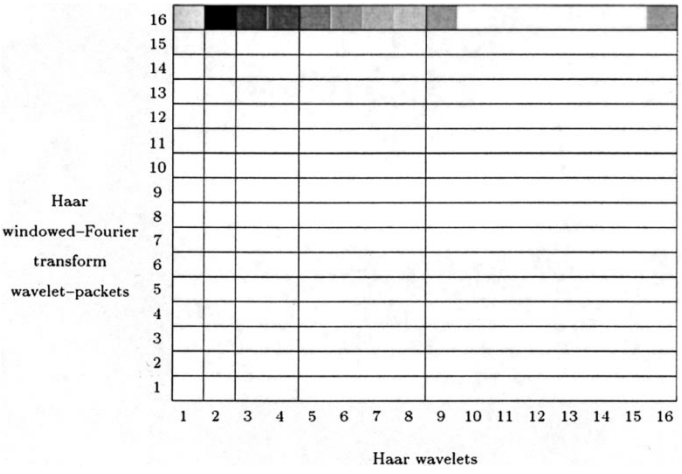

(b)

Fig. 6. Selected elements from the two-stage overcomplete dictionary for the scattering problem illustrated in Fig. 3, with incidence angle of 60°, after 25 iterations. (a) Haar wavelet transformation at both stages. (b) Haar wavelet transformation at first stage and Haar WF transformation at second stage.

Haar wavelet transformation then, at the second stage, the Haar WF transformation. Thus, in both figures the abscissas refer to the set of 16 wavelet functions that spans the surface current on each and every strip, independently. These functions are numbered as shown in Fig. 9(a). This figure presents a wavelet decomposition of the combined space (spatial location—spatial frequency), while Fig. 9(b) presents a decomposition of the combined space into the same number of WF basis functions. The ordinates refer to the second transformation stage, which is Haar wavelet transformation in the case of Fig. 6(a) and Haar WF transformation in the case of Fig. 6(b). For the latter, the elements are numbered in ascending order according to the number of zero-crossings, as shown in Fig. 9(b). The selected basis for the scattering problem in hand is represented by the shaded squares in both figures. Note that the gray-level scale may be used to compare the relative magnitude of each basis element only within the limits of each figure. Finally, note that there are 256 squares in each figure as the current over each strip is spanned by 16 wavelets and there are altogether 16 strips in

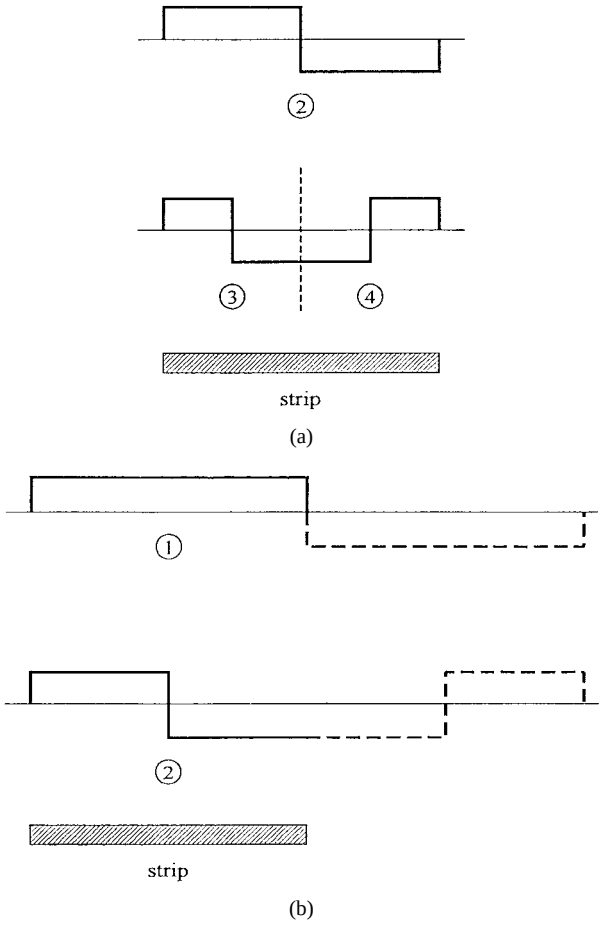

Fig. 7. The dominant functions in the expansion of the induced current density on each conducting strip, for the scattering problem illustrated in Fig. 3, for two angles of incidence: (a) $\Phi_0 = 60°$, hence dominant expansion functions whose superpositions trace a full cycle over each strip; and (b) $\Phi_0 = 75.5°$, hence dominant expansion functions trace only half a cycle over each strip. The dotted lines in (b) describe the imaginary continuation of the half-cycle expansion functions to the complete cycle. The circled numbers refer to the serial numbers of the wavelet functions, as defined in Fig. 9(a).

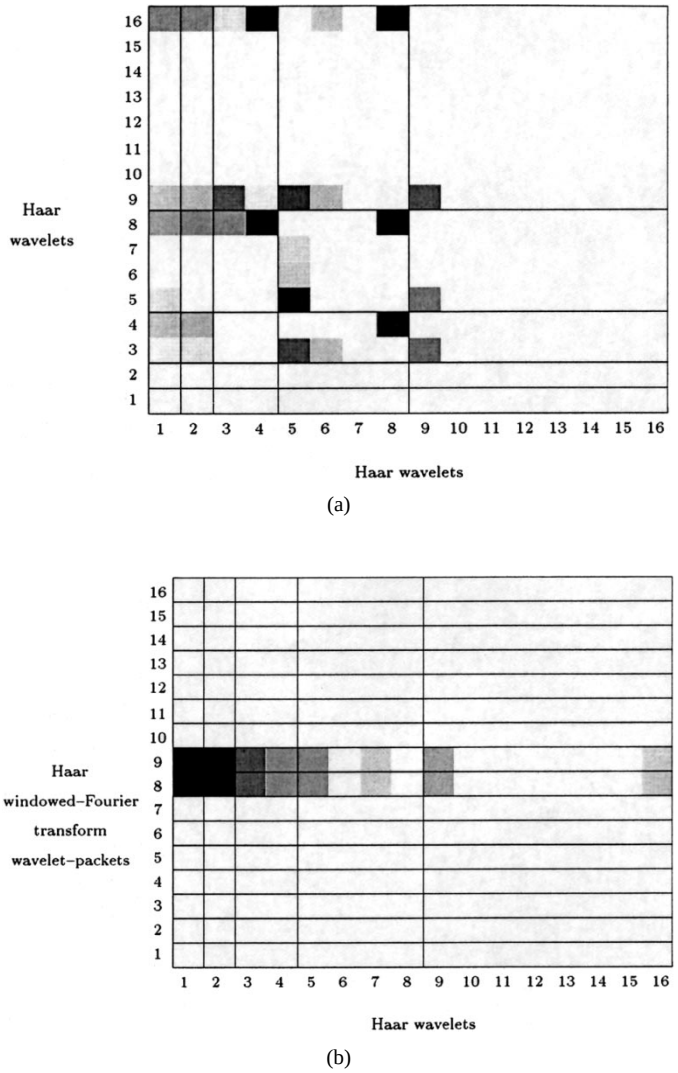

Fig. 8. Selected elements from the two-stage overcomplete dictionary for the scattering problem illustrated in Fig. 3, with incidence angle of 75.5°, after 25 iterations. (a) Haar wavelet transformation at both stages. (b) Haar wavelet transformation at first stage and Haar WF transformation at second stage.

the array. However, no more than a total of 256 squares will be simultaneously shaded in both figures, as an expansion set can not exceed 256 functions. The figures show the selection after 25 iterations (100 expansion functions), when the error in the surface current as defined by (14) drops below 1% for the first time. Referring to Fig. 6(a), one may notice the two dominant columns at unit cell-level wavelet functions number eight and 16. These two wavelet functions span the current at the right edge of each strip. Since periodicity breaks down at the vicinity of the array edges and the coefficients of these wavelets start varying significantly from strip to strip, their array factor is spanned by wavelets and not by WF functions. Fig. 6(b) reveals the periodic features of the current. Since the phase completes a 2π-cycle from one strip to the other, the Haar WF with 15 zero-crossings dominates over the array factor. The phase progression over each strip is spanned by the lowest level wavelet functions [square (2,16) in Fig. 6(b)] which can be interpreted as a single cycle of the sine function, and by the two wavelets of the consecutive scale, [squares (3,16) and (4,16) in Fig. 6(b)], that when properly combined, form the corresponding cosine function as shown in Fig. 7(a).

Fig. 8(a) and (b) presents the selection of expansion functions after 25 iterations for a similar problem in which the incident angle $\Phi_0 = 75.5°$. In this case, it takes two adjacent unit cells to complete a full 2π-cycle. Therefore the frequency of the dominant Haar WF functions is reduced by a half, as shown in Fig. 8(b). Hence, a doublet consisting of sine-like and cosine-like functions is required for properly representing the phase progression of the induced current, and consequently the array factors of the periodic strip-level wavelets shown in Fig. 8(b) are characterized by a corresponding doublet comprising consecutive WF functions. More specifically, note that the dominant functions on each strip are the scaling function [squares (1,8) and (1,9) in Fig. 8(b)], which is constant over each strip, and the lowest level Haar wavelet function [squares (2,8) and (2,9) in Fig. 8(b)]. The scaling function can be viewed as half a cycle of a sine function with a 4λ cycle while the lowest level wavelet can be interpreted as half a cycle of a 4λ cycle cosine function, as shown in Fig. 7(b). The selected combination of these functions naturally accounts

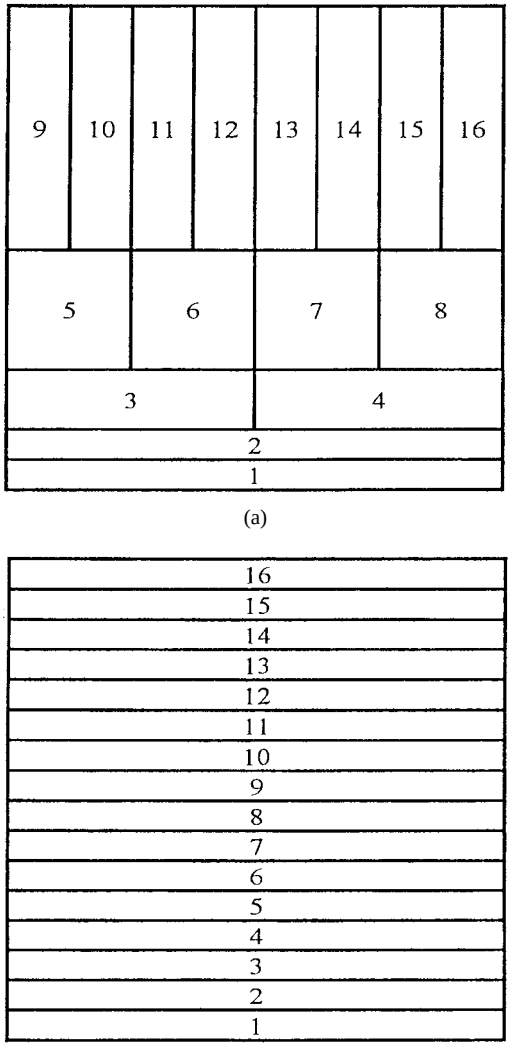

Fig. 9. The key map for (a) wavelet and (b) WF decomposition of the combined space.

for the $k_0 d \cos\Phi_0 = \frac{2\pi}{\lambda} \times 2\lambda \times \cos(75.5^\circ) = \pi$ radian phase change across each strip.

V. Summary and Conclusions

This paper focused on enhancing the compression of the impedance matrix in method of moments solutions of problems of scattering by truncated arrays. We have demonstrated the advantage of an iterative selection of expansion functions from a set of functions constructed via a two-stage Haar wavelet-packet transformation. This two-stage transformation exploits the inherent features of a finite array. The transformation first analyzes the structure at a cell-level and in turn it binds together identical functions from different cells in a way similar to extracting an array factor. Noting that a finite array is not perfectly periodic, the second transformation stage has been modified to yield an overcomplete dictionary comprising both localized and periodic expansion functions. Two numerical examples of scattering by a truncated periodic array have been studied to show the advantages of the proposed method.

Acknowledgment

This study was performed as part of a research project on satellite communication performed under the auspices of the S. Neeman Institute for Advanced Studies in Science and Technology.

References

[1] T. Cwik and R. Mittra, "The effects of the truncation and curvature of periodic surfaces: A strip grating," *IEEE Trans. Antennas Propagat.*, vol. 36, May 1988.
[2] E. G. Johnson and C. G. Christodoulou, "Electromagnetic scattering from aperiodic strip gratings," *J. Electromagn. Waves Applicat.*, vol. 6, no. 2, pp. 219–234, 1992.
[3] L. P. Felsen and L. Carin, "Diffraction theory of frequency and time-domain scattering by weakly aperiodic truncated thin-wire gratings," *J. Opt. Soc. Amer. A*, vol. 11, no. 4, Apr. 1994.
[4] B. Z. Steinberg and Y. Leviatan, "On the use of wavelet expansions in the method of moments," *IEEE Trans. Antennas Propagat.*, vol. 41, pp. 610–619, May 1993.
[5] Z. Baharav and Y. Leviatan, "Impedance matrix compression with the use of wavelet expansions," *Microwave Opt. Technol. Lett.*, vol. 12, no. 3, pp. 268–272, Aug. 1996.
[6] Z. Baharav and Y. Leviatan, "Impedance matrix compression using adaptively-constructed basis functions," *IEEE Trans. Antennas Propagat.*, vol. 44, pp. 1231–1238, Sept. 1996.
[7] Z. Baharav and Y. Leviatan, "Impedance matrix compression (IMC) using iteratively selected wavelet basis for MFIE formulations," *Microwave Opt. Technol. Lett.*, vol. 12, no. 3, pp. 145–150, June 1996.
[8] Z. Baharav and Y. Leviatan, "Impedance matrix compression (IMC) using iteratively selected wavelet-basis," *IEEE Trans. Antennas Propagat.*, vol. 46, pp. 226–233, Feb. 1998.
[9] Z. Baharav and Y. Leviatan, "Wavelets in electromagnetics: The impedance matrix compression (IMC) method," *Int. J. Numer. Modeling*, vol. 11, pp. 69–84, Feb. 1998.
[10] Y. Shifman and Y. Leviatan, "Iterative selection of expansion functions from an overcomplete dictionary of wavelet packets for impedance matrix compression," *J. Electromagn. Waves Applicat.*, vol. 12, pp. 1403–1421, 1998.
[11] A. J. Poggio and E. K. Miller, "Integral equation solutions for three-dimensional scattering problems," *Computer Techniques for Electromagnetics*, R. Mittra, Ed. Oxford, U.K.: Pergamon, 1973, pp. 159–264.
[12] S. G. Mallat and Z. Zhang, "Matching pursuit with time-frequency dictionaries," *IEEE Trans. Signal Processing*, vol. 41, pp. 3397–3415, Dec. 1993.

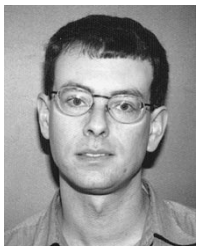

Yair Shifman (S'97) received the B.Sc. and M.Sc. degrees in electrical engineering from the Technion—Israel Institute of Technology, Haifa, Israel, in 1993 and 1998, respectively. He is currently pursuing the Ph.D. degree in electrical engineering at the Technion.

Zachi Baharav (SM' 99), for a photograph and biography, see p. 1238 of the September 1996 issue of this Transactions.

Yehuda Leviatan (S'81–M'86–SM'88–F'98), for a photograph and biography, see p. 1238 of the September 1996 issue of this Transactions.